

Boosting Open-Domain Continual Learning via Leveraging Intra-domain Category-aware Prototype

Yadong Lu¹, Shitian Zhao¹, Boxiang Yun¹, Dongsheng Jiang², Yin Li², Qingli Li¹, Yan Wang^{1*}

¹Shanghai Key Laboratory of Multidimensional Information Processing, East China Normal University

²Huawei Cloud

{yadonglu,10202140413,52265904012}@stu.ecnu.edu.cn, dongsheng_jiang@outlook.com, sherrylee90@163.com, qlli@cs.ecnu.edu.cn, ywang@cee.ecnu.edu.cn

Abstract

Despite recent progress in enhancing the efficacy of Open-Domain Continual Learning (ODCL) in Vision-Language Models (VLM), failing to (1) correctly identify the Task-ID of a test image and (2) use only the category set corresponding to the Task-ID, while preserving the knowledge related to each domain, cannot address the two primary challenges of ODCL: forgetting old knowledge and maintaining zero-shot capabilities, as well as the confusions caused by category-relatedness between domains. In this paper, we propose a simple yet effective solution: leveraging intra-domain category-aware prototypes for ODCL in CLIP (DPeCLIP), where the prototype is the key to bridging the above two processes. Concretely, we propose a training-free Task-ID discriminator method, by utilizing prototypes as classifiers for identifying Task-IDs. Furthermore, to maintain the knowledge corresponding to each domain, we incorporate intra-domain category-aware prototypes as domain prior prompts into the training process. Extensive experiments conducted on 11 different datasets demonstrate the effectiveness of our approach, achieving 2.37% and 1.14% average improvement in class-incremental and task-incremental settings, respectively. Code will be available at <https://github.com/DeepMed-Lab-ECNU/DPeCLIP>.

Introduction

Continual learning (CL) (Dhar et al. 2019; Rebuffi et al. 2017) aims to enable models to continually acquire new knowledge. In recent years, CL has gained significant attention and been applied in various fields, including autonomous driving and medical diagnosis. However, traditional continual learning methods are largely limited to single-domain data, failing to effectively address the complexities of real-world scenarios. In practice, data often come from multiple domains, and there may be significant differences between these domains.

To address this issue, open-domain continual learning (ODCL) (Zheng et al. 2023; Li et al. 2024) has been explored by many recent researchers (Zheng et al. 2023; Yu et al. 2024; Li et al. 2024). The ODCL task utilizes Vision-Language Model (VLM) (Jia et al. 2021; Li et al. 2022; Radford et al. 2021) to linearly learn data from different

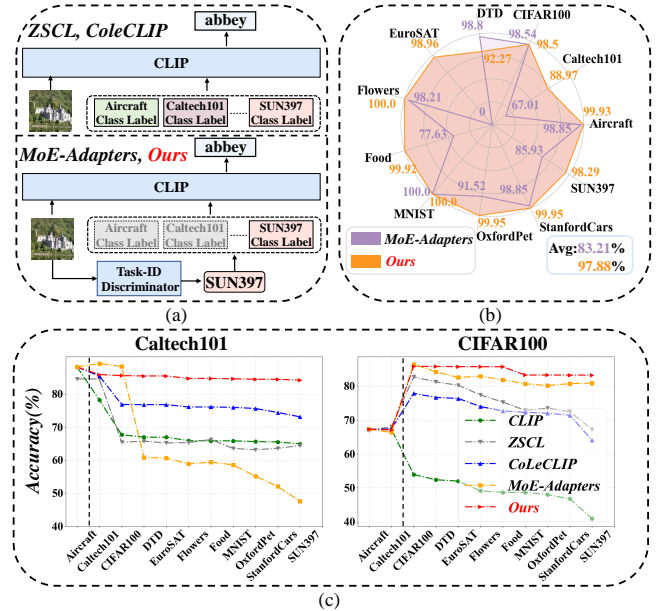


Figure 1: (a) Comparisons of two approaches for solving the ODCL-CIL task: The first uses all seen categories for classification, while the second selects the corresponding categories for classification through a Task-ID discriminator. (b) Comparisons of Task-ID classification accuracy between MoE-Adapters and ours. (c) Comparisons of our and other methods in ODCL-CIL task. The ODCL task requires evaluating both seen and unseen datasets. The black dashed vertical line indicates the test dataset has not been trained on, and it is assessed through the model’s zero-shot capability.

domains, acquiring new domain knowledge while preventing the forgetting of old domain knowledge. Due to the zero-shot classification capability of VLM, ODCL is tested on both seen and unseen domains, necessitating the preservation of VLM’s original zero-shot classification abilities. Similar to traditional continual learning, the ODCL task includes both class-incremental (CIL) and task-incremental (TIL) settings. Compared to ODCL-TIL, ODCL-CIL lacks access to the current image’s Task-ID during inference.

ODCL task faces two significant challenges: (1) **Two types of Forgetting**: Unlike traditional CL task, ODCL

*Corresponding Author: ywang@cee.ecnu.edu.cn.

task faces not only the forgetting of old knowledge but also the forgetting of zero-shot capabilities. (2) **Influence of Category-relatedness Between Domains:** For example, although “wheelchair” in Caltech101 and “chair” in CIFAR100 belong to entirely different categories, their semantic similarity may cause confusion in the ODCL-CIL task, leading to a decrease in dataset performance.

Currently, there are two primary technical approaches to addressing ODCL task, as illustrated in Figure 1(a). For the first approach, during the inference stage, the model utilizes all seen categories to classify the test image regardless of which domain it comes from. ZSCL (Zheng et al. 2023) uses a large reference dataset and distills original CLIP knowledge. However, fully fine-tuning CLIP still leads to significant forgetting. ColeCLIP (Li et al. 2024) seeks to minimize interference from similar categories across different domains by maintaining a vocabulary and employing a carefully crafted task prompt. However, it uses the same text embedding for identical categories across datasets, which leads to inconsistencies due to the lack of updates to the old task prompt, despite employing momentum to slow changes in text embeddings. As shown in Figure 1(c), with the progression of training stages, ColeCLIP exhibits significant catastrophic forgetting issues. These methods try to alleviate the forgetting problem, but since the model cannot access data from multiple domains simultaneously during training, and similar categories from different domains may cause confusion during testing, addressing the category-relatedness problem becomes very challenging.

The second approach involves first determining the Task-ID of the test image using a Task-ID discriminator, and then classifying it using the category set corresponding to the identified Task-ID. For example, MoE-Adapters (Yu et al. 2024) proposes a combination of Auto-Encoder (AE) and AlexNet (Krizhevsky, Sutskever, and Hinton 2012) to identify the Task-ID. Subsequently, it explores the performance of CLIP on the ODCL task by adopting a Mixture of Experts (MoE) (Jacobs et al. 1991) structure. Despite the expert freezing mechanism, the continual updating of experts still results in knowledge forgetting. As shown in Figure 1(b) and (c), the effectiveness of the Task-ID discriminator directly affects the model’s final performance.

Compared to the first approach, the second approach provides a better solution to the category-relatedness issue, as a more robust Task-ID discriminator can effectively tackle this problem. However, even with a well-designed task prompt, using cross-domain information does not alleviate the forgetting issue due to inconsistencies between text embeddings and old task prompts. To address category-relatedness and mitigate forgetting of old domains, two factors should be considered: (1) accurately identifying the Task-ID of a test image and using the corresponding category set, and (2) preserving knowledge relevant to each domain. Additionally, the model must retain the original knowledge of CLIP to maintain strong zero-shot capability.

Based on the above considerations, we propose a simple yet effective solution: leveraging intra-domain category-aware prototypes for ODCL in CLIP (Radford et al. 2021) framework, dubbed as Domain Prototype enhanced CLIP

(DPeCLIP). To maintain the original zero-shot capability of CLIP, we propose to average the original outputs of CLIP’s image and text modalities belonging to the same category within a domain as prototypes. We propose to (1) distinguish the Task-ID of a test image, and (2) preserve the knowledge only related to each domain, where prototypes are the key to bridging them. **Firstly**, we propose a training-free Task-ID discriminator method, by utilizing prototypes as classifiers for identifying Task-IDs. Compared to MoE-Adapters, our method significantly improves Task-ID judgment accuracy without introducing additional training parameters. **Secondly**, to maintain the knowledge corresponding to each domain, we incorporate intra-domain category-aware prototypes as domain prior prompts into training process. For the text branch, we propose a text self-attention module which encodes the relationships of categories within a domain as prompts into the text branch. For the image branch, unlike the text branch, we introduce an image cross-attention module which uses instance-level image embeddings to query category-level prototypes. This ensures that the instance prompt carries information about the relationships between various categories, enabling the learned prompt to encapsulate both domain and instance information.

Overall, our contributions can be summarized below:

- We propose a training-free Task-ID discriminator method that utilizes domain-specific, category-aware prototypes as classifiers to effectively distinguish test images from the original domain.
- We incorporate intra-domain category-aware prototypes as domain prior prompts into the training process to maintain the knowledge corresponding to each domain.
- Through comprehensive experiments on 11 datasets, we demonstrate our method achieves state-of-the-art performance in both ODCL-CIL and ODCL-TIL settings, with 4.90% and 3.33% improvement in *Last* and *Forgetting* metrics for ODCL-CIL task, compared to the 2nd best.

Related Work

Continual Learning

To address the issue of catastrophic forgetting, continual learning can be broadly categorized into three primary approaches: replay-based methods (Bang et al. 2021; Chaudhry et al. 2018; Rebuffi et al. 2017; Lopez-Paz and Ranzato 2017; Prabhu, Torr, and Dokania 2020; Shin et al. 2017), regularization-based methods (Kirkpatrick et al. 2017; Zenke, Poole, and Ganguli 2017; Li and Hoiem 2017; Dhar et al. 2019; Douillard et al. 2020; Hou et al. 2019), and parameter expansion-based methods (Gao et al. 2023; Smith et al. 2023; Wang et al. 2022a; Yan, Xie, and He 2021; Zhou et al. 2022; Wang et al. 2022b,c; Wang, Huang, and Hong 2022). Replay-based methods maintain a buffer of previously encountered data and leverage this replay buffer during the learning of new data to retain the original knowledge. Regularization-based methods aim to preserve prior knowledge by constraining the direction of model updates. Parameter expansion-based methods mitigate forgetting by expanding the model’s architecture to accommo-

date new tasks. Recently, several parameter-efficient fine-tuning (PEFT) based on parameter expansion methods have emerged, such as Low-Rank Adaptation (LoRA) (Hu et al. 2021), prompt-based methods (Lester, Al-Rfou, and Constant 2021), and adapter methods (Houlsby et al. 2019). DualPrompt (Wang et al. 2022b) further mitigates catastrophic forgetting by employing both general and specific prompts. CODA-Prompt (Smith et al. 2023) extends this approach by increasing the scale of prompts and utilizing more prompts simultaneously through a weighting mechanism. LAE (Gao et al. 2023) explores the use of three PEFT methods by implementing both online and offline update strategies.

Continual Learning of CLIP

Currently, numerous studies focus on the performance of CLIP in continual learning, which can be divided into two categories: traditional continual learning (Ding et al. 2022; Zhou et al. 2023; Wang, Huang, and Hong 2022) and ODCL tasks (Zheng et al. 2023; Yu et al. 2024; Li et al. 2024).

Traditional approaches using CLIP (Ding et al. 2022; Zhou et al. 2023; Wang, Huang, and Hong 2022) still focus on a single domain, with the model being simply replaced by CLIP, which does not meet the needs of real life.

ZSCL (Zheng et al. 2023), as the first method proposed for open-domain tasks, balances newly learned knowledge and old knowledge through feature-level distillation with an external dataset. MoE-Adapters (Yu et al. 2024) improve performance in ODCL task by training corresponding AE for Task-ID identification and using a MoE structure. CoLe-CLIP (Li et al. 2024) extends open-domain tasks, by maintaining a vocabulary and designing skillfully task prompts to store task-specific knowledge, but this approach inevitably leads to performance degradation in the ODCL-CIL task.

Methodology

Preliminaries

CLIP CLIP is a model endowed with zero-shot classification capabilities, comprising an image encoder $\mathcal{I}(\cdot)$ and a text encoder $\mathcal{T}(\cdot)$. To employ the CLIP model for classification tasks, an image x is first processed through the image encoder to extract image features. The target classes $\{c^1, c^2, \dots, c^J\}$ for classification are converted into corresponding textual descriptions $\{\hat{c}^1, \hat{c}^2, \dots, \hat{c}^J\}$ using a template such as “a photo of a <category>”, where J represents the total number of categories. These textual descriptions are then fed into CLIP text encoder to generate text features. The cosine similarity between the text features and the image features is computed, and the candidate category with the highest similarity is selected as the classification result.

ODCL For the ODCL tasks, the model is required to sequentially learn from N distinct datasets (domains). The primary objective of this task is to enhance the recognition of new categories while maintaining the ability to recognize previously learned categories. Given N datasets, $\{\mathcal{D}_1, \mathcal{D}_2, \dots, \mathcal{D}_N\}$, as the model learns these datasets linearly, after learning the n th dataset \mathcal{D}_n , it is expected to show good classification capability on the previously learned datasets $\{\mathcal{D}_1, \mathcal{D}_2, \dots, \mathcal{D}_n\}$. At the same time, the

model aims to preserve its zero-shot classification ability for the unlearned datasets $\{\mathcal{D}_{n+1}, \mathcal{D}_{n+2}, \dots, \mathcal{D}_N\}$.

To evaluate the model’s performance, we consider two inference settings: task-incremental (ODCL-TIL) and class-incremental (ODCL-CIL). In ODCL-TIL, the Task-ID is known during inference, enabling the use of the corresponding category set for the test image. In contrast, ODCL-CIL does not provide access to the Task-ID, requiring the use of all seen categories for classification.

Overview of DPeCLIP

Figure 2 illustrates the overall architecture of our method. Our method consists of three parts: (a) Prototypes Calculation Stage, (b) Training Stage, and (c) Inference Stage. In the Prototypes Calculation Stage, we utilize the CLIP image encoder to extract image features of training images belonging to the j th category within n th domain and average them to obtain the mean image feature \bar{I}_n^j . Likewise, we use the CLIP text encoder to extract text features, combined with CLIP templates. By averaging these text features, we obtain the average text feature \bar{T}_n^j . Finally, by performing element-wise summation of \bar{I}_n^j and \bar{T}_n^j , we derive one intra-domain category-aware prototype P_n^j .

During the training stage, we propose domain prior prompts through two sub-modules: Text Self-Attention (TSA) and Image Cross-Attention (ICA), conditioned on the prototypes as input. In addition, we also learn the shared information for each domain through the general prompts. In this process, both domain prior prompts and the general prompts are updated using cross-entropy loss.

During the inference stage, we first utilize the domain prototypes to determine the Task-ID. Then, based on the identified Task-ID, we select the corresponding TSA, ICA modules, general prompts, and the category set associated with the Task-ID from the domain prior prompt pool, which contain all trained components, to classify the test image.

Prototype Calculation Stage

To obtain intra-domain category-aware prototypes for ODCL, we extract prototypes from the training set using the original CLIP model, as shown in Figure 2(a). Specifically, for the j th category in \mathcal{D}_n , containing M training images, the image prototype \bar{I}_n^j can be calculated via: $\bar{I}_n^j = \frac{\sum_{m=1}^M \mathcal{I}(x_n^{j,m})}{M}$, where $x_n^{j,m}$ means the m th image belonging to the j th category of \mathcal{D}_n .

We adopt different templates provided by CLIP to generate various textual descriptions for a category name. For the j th category in the n th domain c_n^j , the textual description generated by the z th template is denoted as $\hat{c}_n^{j,z}$, the templates come from the original CLIP. Then the text prototype \bar{T}_n^j is calculated by: $\bar{T}_n^j = \frac{\sum_{z=1}^Z \mathcal{T}(\hat{c}_n^{j,z})}{Z}$, where Z represents the total number of templates.

Then, we obtain the intra-domain category-aware prototypes P_n^j by element-wise summation of \bar{I}_n^j and \bar{T}_n^j .

Training Stage

Text Branch For the text encoder $\mathcal{T}(\cdot)$, we provide the relationships between different categories within the domain

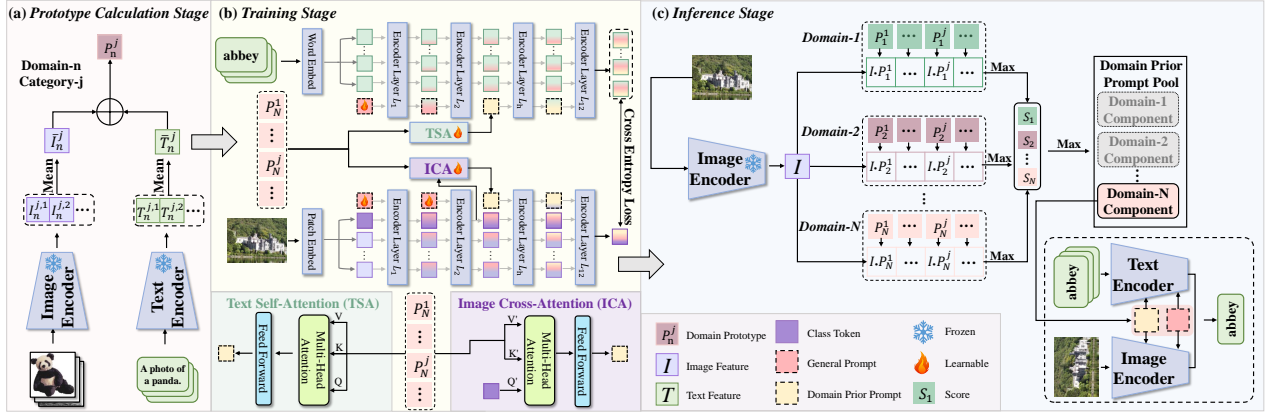


Figure 2: Domain Prototype enhanced CLIP (DPeCLIP) framework, consisting of three stages: (a) Prototype Calculation, where category-aware prototypes are extracted using the original CLIP. (b) Training, where we propose Text Self-Attention (TSA) and Image Cross-Attention (ICA) to provide domain prior prompts, with prototypes as input. (c) Inference, where we use the prototypes to determine Task-IDs for test images and employ the corresponding domain components for classification.

through the domain prior prompt, while learning the general information of the domain through the general prompt, thereby enhancing the model’s classification performance, as shown in Figure 2(b).

We denote the category name of the j th category in \mathcal{D}_n as c_n^j . c_n^j is then processed through CLIP word embedding layer to obtain the text tokens $[t_1^{(1)}, t_2^{(1)}, \dots, t_l^{(1)}]$, subscript l represents the length of text tokens and the superscript (1) represents the first layer. In the first layer $\mathcal{T}^{(1)}(\cdot)$ of the text encoder, we use a general prompt $v_g^{(1)}$, where $v_g^{(1)} \in \mathbb{R}^{1 \times d^T}$ and d^T is the dimension of the text token. This prompt is concatenated with the text tokens of different categories. In this process, only $v_g^{(1)}$ is learnable. Then the output of the first text encoder layer is:

$$[t_1^{(2)}, t_2^{(2)}, \dots, t_l^{(2)}, v_g^{(2)}] = \mathcal{T}^{(1)}([t_1^{(1)}, t_2^{(1)}, \dots, t_l^{(1)}, v_g^{(1)}]). \quad (1)$$

Moreover, we propose a category-aware domain prior prompt for the text encoder. Conditioned on the prototype $P_n = [P_n^1, P_n^2, \dots, P_n^S]^T$ as input, where $P_n \in \mathbb{R}^{S \times d^T}$. We propose a Text Self-Attention (TSA) module to generate the domain prior prompt v_p , $v_p \in \mathbb{R}^{S \times d^T}$. The TSA module is depicted in Figure 2 (with Add and Norm omitted). We use the domain prototype P_n to obtain Q , K , and V in TSA through the formula $Q = W_Q \cdot P_n$, $K = W_K \cdot P_n$, $V = W_V \cdot P_n$, thereby obtaining v_p .

$$\text{Attention}(Q, K, V) = \text{softmax}\left(\frac{QK^T}{\sqrt{d^T}}\right) \cdot V, \quad (2)$$

$$v_p = \text{FFD}(\text{Attention}(Q, K, V)), \quad (3)$$

where W_Q , W_K and $W_V \in \mathbb{R}^{d^T \times d^T}$ are learnable projection matrices, and FFD represents Feed Forward layer.

These domain prior prompts v_p replace the general prompt in the h -th layer of the text encoder. Thus, the output of the h th text encoder layer is:

$$\begin{aligned} & [t_1^{(h+1)}, t_2^{(h+1)}, \dots, t_l^{(h+1)}, v_p^{(h+1)}] \\ & = \mathcal{T}^{(h)}([t_1^{(h)}, t_2^{(h)}, \dots, t_l^{(h)}, v_p]). \end{aligned} \quad (4)$$

Image Branch As shown in Figure 2(b), similar to the text branch, we use the general prompt to learn the general information of the domain for image encoder $\mathcal{I}(\cdot)$. In addition, we utilize the ICA module to generate the instance-level domain prior prompt, thereby providing both domain and instance information simultaneously. Specifically, the image passes through the patch embedding layer to obtain image tokens $[cls^{(1)}, i_1^{(1)}, \dots, i_{l'}^{(1)}]$, where $cls^{(1)}$ is the class token in the first layer and subscript l' is the number of image tokens. In the first $h - 1$ layers of the image encoder, we concatenate a general prompt e_g , where $e_g \in \mathbb{R}^{1 \times d^I}$ with the image tokens at each layer, and d^I means the dimension of image token. For example, for the $h - 1$ layer $\mathcal{I}^{(h-1)}(\cdot)$ of image encoder, the general prompt $e_g^{(h-1)}$ is used by following:

$$\begin{aligned} & [cls^{(h)}, t_1^{(h)}, \dots, t_{l'}^{(h)}, e_g^{(h)}] = \\ & \mathcal{I}^{(h-1)}([cls^{(h-1)}, t_2^{(h-1)}, \dots, t_{l'}^{(h-1)}, e_g^{(h-1)}]). \end{aligned} \quad (5)$$

In this process, all $e_g^{(1)}, e_g^{(2)}, \dots, e_g^{(h-1)}$ are learnable.

In addition to the general prompt, we provide instance-level domain prior prompt for the image encoder. Using the prototype P_n as input, we propose an Image Cross-Attention (ICA) module to dynamically generate instance-level prompt. The class token $cls^{(h)}$ from the h th layer of the image encoder serves as the Q' , while the domain prototype serves as K' and V' through the formula $Q' = W'_Q \cdot cls^{(h)}$, $K' = W'_K \cdot P_n$, $V' = W'_V \cdot P_n$, where $W'_Q \in \mathbb{R}^{d^I \times d^I}$, W'_K and $W'_V \in \mathbb{R}^{d^I \times d^T}$ are learnable projection matrices in the image branch, yielding the domain prior prompt e_p , where $e_p \in \mathbb{R}^{1 \times d^I}$.

After training each domain, we save the general prompts, TSA, and ICA modules as the domain component into the domain prior prompt pool for inference.

Task	Method	Aircraft	Caltech101	CIFAR100	DTD	EuroSAT	Flowers	Food	MNIST	OxfordPet	Cars	SUN397	Mean	
ODCL-CIL	Last	CODA-Prompt	12.81	65.38	63.49	53.83	56.91	56.64	83.31	83.99	76.83	53.65	75.13	62.00
		LAE	13.65	83.06	66.88	59.20	36.61	48.95	84.08	94.22	75.44	42.69	78.69	62.14
		CLIP	24.39	63.65	40.99	39.26	52.98	70.04	88.40	39.56	88.85	64.52	63.28	57.81
		ZSCL	42.54	64.40	67.24	54.84	89.70	90.37	91.73	95.76	93.38	85.20	78.30	77.59
		MoE-Adapters	34.11	47.58	80.88	75.48	0.00	93.02	70.78	99.35	86.40	79.80	68.89	66.93
		CoLeCLIP	48.09	73.10	65.22	69.63	83.98	96.21	90.88	94.56	93.54	82.61	79.34	79.74
	DPeCLIP	49.86	84.21	83.23	71.06	97.01	95.77	92.02	99.40	93.89	84.47	80.17	84.64	
	Forgetting	CODA-Prompt	20.18	73.61	73.43	62.75	84.66	69.79	87.42	83.00	80.96	65.57	75.13	70.59
		LAE	17.07	85.58	75.64	67.70	64.90	70.45	87.63	96.64	86.54	62.49	78.69	72.12
		CLIP	24.42	66.26	48.92	41.03	53.09	70.04	88.43	39.56	88.93	64.53	63.28	58.95
		ZSCL	46.32	66.72	75.87	60.61	94.85	91.75	91.83	94.30	94.14	85.48	78.30	80.02
		MoE-Adapters	37.17	63.06	82.26	76.18	0.00	93.60	71.03	99.42	86.97	80.15	68.89	68.97
		CoLeCLIP	48.24	76.72	73.15	73.51	89.74	96.21	91.02	94.56	93.76	82.64	79.34	81.72
	DPeCLIP	49.86	84.97	84.63	72.96	97.36	95.77	92.03	99.40	93.93	84.48	80.17	85.05	
	Avg	CLIP	24.42	68.21	52.28	42.14	53.66	70.27	88.58	52.20	89.07	64.55	65.25	60.97
		ZSCL	46.32	68.34	74.34	56.29	79.10	81.42	89.52	73.96	89.01	64.35	67.49	71.83
		MoE-Adapters	37.17	65.34	79.45	67.59	19.66	83.13	80.53	73.98	88.48	67.51	65.34	66.19
		CoLeCLIP	48.24	77.76	71.69	65.65	76.78	83.76	89.64	72.22	90.33	67.97	66.40	73.68
DPeCLIP	49.86	85.26	81.45	65.25	81.58	84.31	89.93	73.97	90.37	68.30	66.17	76.05		
ODCL-TIL	Last	CODA-Prompt	43.59	92.97	74.47	75.21	92.57	93.07	90.25	98.61	92.75	83.80	78.75	83.28
		LAE	49.14	93.84	80.53	75.43	90.63	87.07	88.94	98.64	92.94	81.36	80.08	83.51
		CLIP	24.42	87.79	67.36	45.11	54.65	70.53	88.70	59.43	89.13	64.56	65.45	65.19
		ZSCL	42.60	92.40	81.37	70.64	94.63	90.58	91.76	98.64	93.70	85.21	79.69	83.75
		MoE-Adapters	34.59	94.70	82.69	76.91	97.65	94.76	91.86	99.35	94.74	80.86	80.54	84.42
		CoLeCLIP	48.66	94.93	78.78	78.35	88.85	96.29	91.10	97.63	94.39	82.73	80.15	84.71
	DPeCLIP	49.86	95.62	85.79	78.61	98.38	95.77	92.11	99.40	93.97	84.49	81.69	86.89	
	Forgetting	CODA-Prompt	47.49	92.84	78.23	76.40	94.51	95.23	90.20	98.55	93.12	83.99	78.75	84.48
		LAE	53.69	94.06	80.50	76.72	93.54	90.34	89.46	98.97	93.42	84.38	80.08	85.02
		CLIP	24.42	87.79	67.36	45.11	54.65	70.53	88.70	59.43	89.13	64.56	65.45	65.19
		ZSCL	46.35	93.45	82.67	71.56	96.15	91.98	91.84	98.78	94.36	85.49	79.69	84.76
		MoE-Adapters	37.38	94.41	83.56	77.17	97.79	95.32	91.88	99.42	94.57	81.01	80.54	84.82
		CoLeCLIP	48.66	94.96	79.16	78.35	93.25	96.29	91.10	97.63	94.39	82.73	80.15	85.15
	DPeCLIP	49.86	95.62	85.79	78.61	98.38	95.77	92.11	99.40	93.97	84.49	81.69	86.89	
	Avg	CLIP	24.42	87.79	67.36	45.11	54.65	70.53	88.70	59.43	89.13	64.56	65.45	65.19
		ZSCL	46.35	92.64	79.91	64.26	79.93	81.54	89.53	75.59	89.07	64.35	67.62	75.52
		MoE-Adapters	37.38	93.85	80.51	68.31	81.89	84.07	90.01	73.98	90.55	67.67	66.40	75.87
		CoLeCLIP	48.66	94.34	76.61	69.17	79.01	83.81	89.67	73.33	90.50	67.98	66.48	76.32
DPeCLIP	49.86	94.94	82.40	69.36	82.23	84.31	89.97	73.97	90.38	68.30	66.31	77.46		

Table 1: Last, Forgetting, and Avg (%) in ODCL-CIL and ODCL-TIL. CODA-Prompt and LAE are not applicable to Avg.

Inference Stage

For a test image from previously seen domains in ODCL-CIL, we first employ the prototype Task-ID discriminator to determine its Task-ID, as shown in Figure 2(c). For a test image x , we use $\mathcal{I}(x)$ to extract the image feature I . We then calculate the cosine similarity between I and the learned domain prototypes of different domains. For each domain, we select the highest similarity score, and then compare the similarities scores across different domains to obtain the Task-ID. Next, we select the corresponding domain component from the domain prior prompt pool. Classification of the test image is then performed within the category set associated with the identified Task-ID domain and domain component.

For a test image from unseen domains, we adopt an approach similar to ColeCLIP. We use CLIP to perform zero-shot classification on the image from unseen domains. However, if the unseen dataset contains categories that have been previously seen, we will query the previously seen domains in which the corresponding categories appear. We then use the components associated with those domains to compute the cosine similarity for the respective categories. The category with the highest similarity is selected as the result. Finally, we compare this with the cosine similarity of CLIP for unseen categories, choosing the largest as the final result.

Experiments

Experiments Setup

Datasets The ODCL task comprises 11 datasets across various domains, including Aircraft (Maji et al. 2013), Caltech101 (Fei-Fei, Fergus, and Perona 2004), CIFAR100 (Krizhevsky and Hinton 2009), DTD (Cimpoi et al. 2014), EuroSAT (Helber et al. 2019), Flowers (Nilsback and Zisserman 2008), Food (Bossard, Guillaumin, and Van Gool 2014), MNIST (Deng 2012), OxfordPet (Parkhi et al. 2012), StanfordCars (Krause et al. 2013), and SUN397 (Xiao et al. 2010). The sequence in the ODCL task typically follows two orders, as previously adopted in the works of ZSCL (Zheng et al. 2023), ColeCLIP (Li et al. 2024). The Order-I arranges the datasets alphabetically by their names, while the Order-II is determined randomly. The experimental results presented in the main text are based on the Order-I, whereas the supplementary materials provide results based on the Order-II.

Implementation Details Building upon the previous research by ZSCL and ColeCLIP, we adopt the CLIP-ViT-B/16 (Radford et al. 2021) model as the foundational architecture for the ODCL task. All experimental settings strictly follow ColeCLIP (Li et al. 2024), more detailed descriptions are provided in the supplementary materials.

For the text encoder, we employ a single-layer learnable prompt as the general prompt integrated with a TSA module. The domain prior prompt generated by the TSA module replaces the original prompt in the 8-th layer. For the image encoder, we utilize a 7-layer deep learnable prompts as general

Method	Caltech101	CIFAR100	DTD	EuroSAT	Flowers	Food	MNIST	OxfordPet	Cars	SUN397	Mean
CLIP	88.19	67.31	44.68	55.26	70.22	88.50	59.45	89.04	64.71	65.16	69.25
ZSCL	84.56	67.45	44.77	51.54	69.02	87.60	62.34	87.08	59.65	66.41	68.04
MoE-Adapters	88.19	66.82	44.68	54.07	70.56	88.44	59.45	89.04	64.71	64.99	69.08
CoLeCLIP	88.19	65.12	44.68	54.10	68.82	88.49	59.45	89.04	64.71	65.11	68.77
DPeCLIP	88.19	67.18	44.68	53.97	70.58	88.19	59.45	89.04	64.71	64.78	69.08

Table 2: *Transfer* results(%) in ODCL task.

PTD	TC	IC	Avg \uparrow	Last \uparrow	Forgetting \uparrow	Transfer \uparrow
-	-	-	61.00	57.87	59.01	69.25
\checkmark			64.06	63.62	63.81	69.25
\checkmark	\checkmark		75.20	83.41	83.79	69.07
\checkmark		\checkmark	73.14	79.48	79.86	69.09
\checkmark	\checkmark	\checkmark	76.05	84.64	85.05	69.08

Table 3: The impact of different module combinations on model performance. PTD is Prototype Task-ID discriminator, TC is text component and IC is image component.

CoOp	LP	TSA	Avg \uparrow	Last \uparrow	Forgetting \uparrow	Transfer \uparrow
\checkmark			70.64	75.80	76.12	69.00
\checkmark	\checkmark		71.76	77.22	77.75	68.90
\checkmark		\checkmark	75.20	83.41	83.79	69.07

Table 4: Analysis on the text branch. CoOp represents learnable prompt in 1th layer. LP is learnable prompt in 8th layer. TSA represents domain prior prompt in 8th layer.

prompts, complemented by an ICA module. The instance-level domain prior prompt generated by ICA replaces the original prompt in the 8-th layer. In line with the prompt length employed in ColeCLIP, we set the prompt length to 1 for both encoders.

Evaluation Metrics Following previous work such as ZSCL, ColeCLIP, we use *Avg*, *Last*, *Transfer*, and *Forgetting* as evaluation metrics to assess performance on the ODCL task. For the n th dataset \mathcal{D}_n , we use A_n , F_n and R_n to represent the mean accuracy, Forgetting and Transfer metrics, respectively. More detailed descriptions are provided in the supplementary materials.

Comparison Methods We select CLIP (Radford et al. 2021), ZSCL, MoE-Adapters (Yu et al. 2024), CODA-Prompt (Smith et al. 2023), LAE (Gao et al. 2023) and ColeCLIP as the baseline methods for comparison. More detailed descriptions can be found in the supplementary materials.

Main Properties

Performance on ODCL-CIL As previously mentioned, ODCL-CIL presents a more challenging task compared to ODCL-TIL due to the absence of Task-ID information during the inference stage. Table 1 ODCL-CIL part provides a comparison between our proposed method DPeCLIP and other approaches, highlighting significant improvements in performance.

Notably, DPeCLIP achieves improvements of 4.90% and 3.33% over CoLeCLIP in the *Last* and *Forgetting* metrics, respectively. For Caltech101 and CIFAR100, which are significantly affected by the category-relatedness issue, the first category of methods, ZSCL and ColeCLIP, exhibited noticeable forgetting phenomena. MoE-Adapters and our method demonstrate that a robust Task-ID discriminator can effectively address the category-relatedness problem. Addition-

VPT	LP	ICA	Avg \uparrow	Last \uparrow	Forgetting \uparrow	Transfer \uparrow
\checkmark			70.15	74.84	75.16	68.12
\checkmark	\checkmark		70.93	75.96	76.30	68.58
\checkmark		\checkmark	73.14	79.48	79.86	69.09

Table 5: Analysis on the image branch. VPT represents learnable prompt in 1-7 layers. LP is learnable prompt in 8th layer. ICA represents domain prior prompt in 8th layer.

Prototype granularity	Avg \uparrow	Last \uparrow	Forgetting \uparrow
Domain-level	67.11	62.32	69.18
Category-level	76.05	84.65	85.05

Table 6: The impact of prototype granularity for the Task-ID discriminator in ODCL-CIL task. Domain-level represents one prototype for each domain, while category-level represents one prototype for each category within each domain.

ally, due to the shortcomings of MoE-Adapters’ Task-ID discriminator, the performance on many datasets is significantly affected, such as Caltech101, EuroSAT, and Food.

Our method shows an enhancement of 2.37% compared to CoLeCLIP in *Avg*. Although MoE-Adapters demonstrates strong performance on the DTD task, it utilizes the AutoEncoder as the Task-ID discriminator, which fails to recognize test images from EuroSAT. Thus, it negatively impacts the overall performance. In comparison, our prototype Task-ID discriminator approach demonstrates exceptional performance in terms of Task-ID identification accuracy, which ultimately enhances the overall model performance.

Performance on ODCL-TIL For the ODCL-TIL task, DPeCLIP continues to demonstrate exceptional performance, as illustrated in Table 1 ODCL-TIL part. In terms of the *Last*, *Forgetting*, and *Avg* metrics, DPeCLIP achieves the highest results, surpassing CoLeCLIP by 2.18%, 1.74%, and 1.14%, respectively. This highlights that DPeCLIP not only excels in addressing the issue of forgetting but also achieves superior learning outcomes across various domain tasks. DPeCLIP effectively balances the trade-off between learning capability and forgetting mitigation.

Transfer Performance Table 2 presents the *Transfer* metric for models on the ODCL-TIL task. ZSCL, by fully fine-tuning the CLIP model, experiences a significant decline in *transfer* performance, with a reduction of 1.21%. CoLeCLIP mitigates this issue by maintaining a large vocabulary, resulting in notable improvements. MoE-Adapters utilizes a MoE structure to retain CLIP’s original knowledge, and it exhibits relatively good performance on the *transfer* metric. In contrast, DPeCLIP introduces domain prototypes as input for the domain prior prompts, aiming to retain the original knowledge of CLIP as much as possible, thereby concurrently outperforming other methods on various other metrics, achieving the same level of performance on the *Trans-*

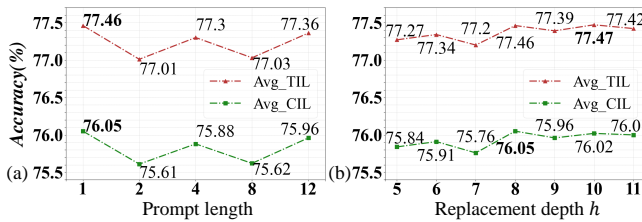


Figure 3: (a) represents the influence of prompt length and (b) represents the influence of prompt replacement depth.

Prototype type	Avg \uparrow	Last \uparrow	Forgetting \uparrow
TP	69.39	72.27	73.91
IP	76.00	84.39	85.03
TP&IP	76.05	84.65	85.05

Table 7: Different types of prototypes for the Task-ID discriminator. TP is text prototype and IP is image prototype.

fers metric as MoE-Adapters, with only a 0.17% reduction.

Analysis and Discussion

Module Analysis We conduct comprehensive ablation experiments on DPeCLIP to assess the impact of different components. Since the ODCL-CIL task better evaluates overall model performance, Table 3 presents results using various components for this task. The first row shows the performance of the original CLIP. By incorporating the prototype Task-ID discriminator without additional training, the *Avg*, *Last*, and *Forgetting* metrics improve significantly by 3.06%, 5.75%, and 4.8%, respectively. This method effectively addresses category-relatedness issues across domains.

TC (Text Component) refers to the general prompt and domain prior prompt generated by the TSA module for the text encoder and IC (Image Component) represents the general prompt and instance-level domain prior prompt generated by the ICA module for the image encoder. Compared to IC, the TC shows a more significant increase in the three main metrics, demonstrating that fine-tuning the text encoder is more effective. Additionally, the domain prior prompt generated from the domain prototype performs well in retaining the original knowledge of CLIP, resulting in only a slight decline in the *Transfer* metric. The integration of the three modules achieves the best performance the three main metrics, with only a very slight decline in the *Transfer* metric. The detailed ablation experiments are presented below.

Effectiveness of TSA Table 4 shows an analysis of TC. Compared to the combination of CoOp and LP, the combination of CoOp and TSA shows significant improvements across all metrics, demonstrating the effectiveness of the domain prior prompt for the text encoder.

Effectiveness of ICA Table 5 presents an analysis of IC. Notably, the combination of VPT and ICA shows significant growth in all metrics, demonstrating that the domain prior prompt retains more of CLIP’s original knowledge compared to the learnable prompt.

Prompt Length Figure 3(a) presents the performance of DPeCLIP with different prompt length. Given the same set-

Prototype type	Transfer \uparrow	ODCL-CIL			ODCL-TIL		
		Avg \uparrow	Last \uparrow	Forgetting \uparrow	Avg \uparrow	Last \uparrow	Forgetting \uparrow
IP	69.05	75.92	84.47	84.89	77.35	86.72	86.72
TP	69.01	75.95	84.55	84.95	77.36	86.77	86.77
IP&TP	69.08	76.05	84.65	85.05	77.46	86.89	86.89

Table 8: Different types of prototype for domain prior prompt. TP is text prototype and IP is image prototype.

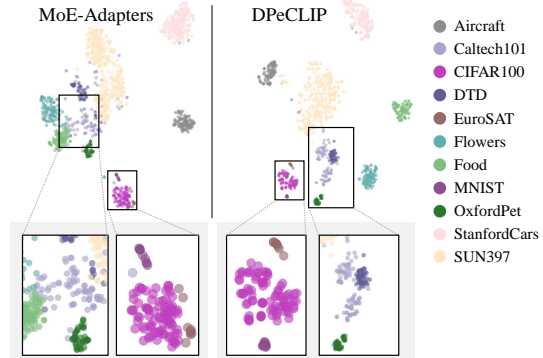


Figure 4: Comparison of t-SNE between MoE-Adapters and our method for the Task-ID discriminator.

tings for hyperparameters, DPeCLIP exhibits the best performance across all metrics when the prompt length is 1.

Replacement Depth Figure 3(b) shows the effects of replacement depth for the domain prior prompt. We experimented with layers 5 to 11 of the encoder as replacement depth. Although the *Transfer* metric performs best when inserted at layer 6, we ultimately chose layer 8 for the best overall performance. We hypothesize that layer 8 allows the model to better balance low-level and high-level features.

Prototype Granularity for the Task-ID Discriminator Table 6 shows the impact of different prototype granularities for the Task-ID discriminator. Compared to domain-level prototypes, category-level prototypes can retain more domain information, resulting in more accurate Task-ID judgments and better model performance.

Prototype Type for the Task-ID Discriminator Table 7 shows the impact of different types of prototypes on the Task-ID discriminator in ODCL-CIL task. Compared to the confusion issues associated with TP, IP better represents domain-level information, resulting in improved performance of the Task-ID discriminator. We found that using IP and TP together can slightly enhance performance, maybe due to complementarity of different prototype.

Prototype Type for the Domain Prior Prompt Table 8 illustrates the influence of different type of prototype for domain prior prompt. It can be observed that using either type of prototype individually can achieve good performance. To provide more comprehensive information, we adopted a combination of TP and IP, achieving the best results.

t-SNE Visualization Figure 4 shows the different distributions between MoE-Adapters and our method for the Task-ID discriminator. MoE-Adapters exhibit significant confusion, whereas our method effectively reduces this confusion. The comparison of the magnified sections further demonstrates the superior performance of DPeCLIP on the Task-ID discriminator task.

Conclusion

In this work, we propose DPeCLIP to address the challenges faced by VLMs in the ODCL task. By utilizing intra-domain category-aware prototypes as a key component, we introduce domain prior prompts to enhance the model’s classification performance while achieving a robust Task-ID discriminator. Extensive experiments demonstrate the effectiveness of our approach.

References

- Bang, J.; Kim, H.; Yoo, Y.; Ha, J.-W.; and Choi, J. 2021. Rainbow memory: Continual learning with a memory of diverse samples. In *Proc. CVPR*, 8218–8227.
- Bossard, L.; Guillaumin, M.; and Van Gool, L. 2014. Food-101—mining discriminative components with random forests. In *Proc. ECCV*, 446–461. Springer.
- Chaudhry, A.; Dokania, P. K.; Ajanthan, T.; and Torr, P. H. 2018. Riemannian walk for incremental learning: Understanding forgetting and intransigence. In *Proc. ECCV*, 532–547.
- Cimpoi, M.; Maji, S.; Kokkinos, I.; Mohamed, S.; and Vedaldi, A. 2014. Describing textures in the wild. In *Proc. CVPR*, 3606–3613.
- Deng, L. 2012. The mnist database of handwritten digit images for machine learning research [best of the web]. *IEEE signal processing magazine*, 29(6): 141–142.
- Dhar, P.; Singh, R. V.; Peng, K.-C.; Wu, Z.; and Chellappa, R. 2019. Learning without memorizing. In *Proc. CVPR*, 5138–5146.
- Ding, Y.; Liu, L.; Tian, C.; Yang, J.; and Ding, H. 2022. Don’t stop learning: Towards continual learning for the clip model. *arXiv preprint arXiv:2207.09248*.
- Douillard, A.; Cord, M.; Ollion, C.; Robert, T.; and Valle, E. 2020. Podnet: Pooled outputs distillation for small-tasks incremental learning. In *Proc. ECCV*, 86–102. Springer.
- Fei-Fei, L.; Fergus, R.; and Perona, P. 2004. Learning generative visual models from few training examples: An incremental bayesian approach tested on 101 object categories. In *Proc. CVPR workshop*, 178–178. IEEE.
- Gao, Q.; Zhao, C.; Sun, Y.; Xi, T.; Zhang, G.; Ghanem, B.; and Zhang, J. 2023. A unified continual learning framework with general parameter-efficient tuning. In *Proc. ICCV*, 11483–11493.
- Helber, P.; Bischke, B.; Dengel, A.; and Borth, D. 2019. Eurosat: A novel dataset and deep learning benchmark for land use and land cover classification. *IEEE Journal of Selected Topics in Applied Earth Observations and Remote Sensing*, 12(7): 2217–2226.
- Hou, S.; Pan, X.; Loy, C. C.; Wang, Z.; and Lin, D. 2019. Learning a unified classifier incrementally via rebalancing. In *Proc. CVPR*, 831–839.
- Houlsby, N.; Giurgiu, A.; Jastrzebski, S.; Morrone, B.; De Laroussilhe, Q.; Gesmundo, A.; Attariyan, M.; and Gelly, S. 2019. Parameter-efficient transfer learning for NLP. In *Proc. ICML*, 2790–2799. PMLR.
- Hu, E. J.; Shen, Y.; Wallis, P.; Allen-Zhu, Z.; Li, Y.; Wang, S.; Wang, L.; and Chen, W. 2021. Lora: Low-rank adaptation of large language models. *arXiv preprint arXiv:2106.09685*.
- Jacobs, R. A.; Jordan, M. I.; Nowlan, S. J.; and Hinton, G. E. 1991. Adaptive mixtures of local experts. *Neural computation*, 3(1): 79–87.
- Jia, C.; Yang, Y.; Xia, Y.; Chen, Y.-T.; Parekh, Z.; Pham, H.; Le, Q.; Sung, Y.-H.; Li, Z.; and Duerig, T. 2021. Scaling up visual and vision-language representation learning with noisy text supervision. In *Proc. ICML*, 4904–4916. PMLR.
- Kirkpatrick, J.; Pascanu, R.; Rabinowitz, N.; Veness, J.; Desjardins, G.; Rusu, A. A.; Milan, K.; Quan, J.; Ramalho, T.; Grabska-Barwinska, A.; et al. 2017. Overcoming catastrophic forgetting in neural networks. *Proceedings of the national academy of sciences*, 114(13): 3521–3526.
- Krause, J.; Stark, M.; Deng, J.; and Fei-Fei, L. 2013. 3d object representations for fine-grained categorization. In *Proc. ICCV workshops*, 554–561.
- Krizhevsky, A.; and Hinton, G. 2009. Learning multiple layers of features from tiny images. *Handbook of Systemic Autoimmune Diseases*, 1(4).
- Krizhevsky, A.; Sutskever, I.; and Hinton, G. E. 2012. ImageNet classification with deep convolutional neural networks. *Proc. NIPS*, 25.
- Lester, B.; Al-Rfou, R.; and Constant, N. 2021. The power of scale for parameter-efficient prompt tuning. *arXiv preprint arXiv:2104.08691*.
- Li, J.; Li, D.; Xiong, C.; and Hoi, S. 2022. Blip: Bootstrapping language-image pre-training for unified vision-language understanding and generation. In *Proc. ICML*, 12888–12900. PMLR.
- Li, Y.; Pang, G.; Suo, W.; Jing, C.; Xi, Y.; Liu, L.; Chen, H.; Liang, G.; and Wang, P. 2024. CoLeCLIP: Open-Domain Continual Learning via Joint Task Prompt and Vocabulary Learning. *arXiv preprint arXiv:2403.10245*.
- Li, Z.; and Hoiem, D. 2017. Learning without forgetting. *IEEE transactions on pattern analysis and machine intelligence*, 40(12): 2935–2947.
- Lopez-Paz, D.; and Ranzato, M. 2017. Gradient episodic memory for continual learning. *Proc. NIPS*, 30.
- Maji, S.; Rahtu, E.; Kannala, J.; Blaschko, M.; and Vedaldi, A. 2013. Fine-grained visual classification of aircraft. *arXiv preprint arXiv:1306.5151*.
- Nilsback, M.-E.; and Zisserman, A. 2008. Automated flower classification over a large number of classes. In *2008 Sixth Indian conference on computer vision, graphics & image processing*, 722–729. IEEE.
- Parkhi, O. M.; Vedaldi, A.; Zisserman, A.; and Jawahar, C. 2012. Cats and dogs. In *Proc. CVPR*, 3498–3505. IEEE.
- Prabhu, A.; Torr, P. H.; and Dokania, P. K. 2020. Gdumb: A simple approach that questions our progress in continual learning. In *Proc. ECCV*, 524–540. Springer.
- Radford, A.; Kim, J. W.; Hallacy, C.; Ramesh, A.; Goh, G.; Agarwal, S.; Sastry, G.; Askell, A.; Mishkin, P.; Clark, J.; et al. 2021. Learning transferable visual models from natural language supervision. In *Proc. ICML*, 8748–8763. PMLR.

Rebuffi, S.-A.; Kolesnikov, A.; Sperl, G.; and Lampert, C. H. 2017. icarl: Incremental classifier and representation learning. In *Proc. CVPR*, 2001–2010.

Shin, H.; Lee, J. K.; Kim, J.; and Kim, J. 2017. Continual learning with deep generative replay. *Proc. NIPS*, 30.

Smith, J. S.; Karlinsky, L.; Gutta, V.; Cascante-Bonilla, P.; Kim, D.; Arbelle, A.; Panda, R.; Feris, R.; and Kira, Z. 2023. Coda-prompt: Continual decomposed attention-based prompting for rehearsal-free continual learning. In *Proc. CVPR*, 11909–11919.

Wang, F.-Y.; Zhou, D.-W.; Ye, H.-J.; and Zhan, D.-C. 2022a. Foster: Feature boosting and compression for class-incremental learning. In *Proc. ECCV*, 398–414. Springer.

Wang, Y.; Huang, Z.; and Hong, X. 2022. S-prompts learning with pre-trained transformers: An occam’s razor for domain incremental learning. *Proc. NIPS*, 35: 5682–5695.

Wang, Z.; Zhang, Z.; Ebrahimi, S.; Sun, R.; Zhang, H.; Lee, C.-Y.; Ren, X.; Su, G.; Perot, V.; Dy, J.; et al. 2022b. Dual-Prompt: Complementary Prompting for Rehearsal-free Continual Learning. *Proc. ECCV*.

Wang, Z.; Zhang, Z.; Lee, C.-Y.; Zhang, H.; Sun, R.; Ren, X.; Su, G.; Perot, V.; Dy, J.; and Pfister, T. 2022c. Learning to prompt for continual learning. In *Proc. CVPR*, 139–149.

Xiao, J.; Hays, J.; Ehinger, K. A.; Oliva, A.; and Torralba, A. 2010. Sun database: Large-scale scene recognition from abbey to zoo. In *Proc. CVPR*, 3485–3492. IEEE.

Yan, S.; Xie, J.; and He, X. 2021. Der: Dynamically expandable representation for class incremental learning. In *Proc. CVPR*, 3014–3023.

Yu, J.; Zhuge, Y.; Zhang, L.; Hu, P.; Wang, D.; Lu, H.; and He, Y. 2024. Boosting continual learning of vision-language models via mixture-of-experts adapters. In *Proc. CVPR*, 23219–23230.

Zenke, F.; Poole, B.; and Ganguli, S. 2017. Continual learning through synaptic intelligence. In *Proc. ICML*, 3987–3995. PMLR.

Zheng, Z.; Ma, M.; Wang, K.; Qin, Z.; Yue, X.; and You, Y. 2023. Preventing zero-shot transfer degradation in continual learning of vision-language models. In *Proc. ICCV*, 19125–19136.

Zhou, D.-W.; Wang, Q.-W.; Ye, H.-J.; and Zhan, D.-C. 2022. A model or 603 exemplars: Towards memory-efficient class-incremental learning. *arXiv preprint arXiv:2205.13218*.

Zhou, D.-W.; Zhang, Y.; Ning, J.; Ye, H.-J.; Zhan, D.-C.; and Liu, Z. 2023. Learning without forgetting for vision-language models. *arXiv preprint arXiv:2305.19270*.